

# Distill and Fine-tune: Effective Adaptation from a Black-box Source Model

Jian Liang<sup>1</sup> Dapeng Hu<sup>1</sup> Ran He<sup>3,4</sup> Jiashi Feng<sup>2,1</sup>

<sup>1</sup> National University of Singapore (NUS) <sup>2</sup> Sea AI Lab (SAIL) <sup>3</sup> Institute of Automation, Chinese Academy of Sciences (UCAS) <sup>4</sup> University of Chinese Academy of Sciences (UCAS)

liangjian92@gmail.com dapeng.hu@u.nus.edu rhe@nlpr.ia.ac.cn elefjia@nus.edu.sg

## Abstract

To alleviate the burden of labeling, unsupervised domain adaptation (UDA) aims to transfer knowledge in previous related labeled datasets (source) to a new unlabeled dataset (target). Despite impressive progress, prior methods always need to access the raw source data and develop data-dependent alignment approaches to recognize the target samples in a transductive learning manner, which may raise privacy concerns from source individuals. Several recent studies resort to an alternative solution by exploiting the well-trained white-box model instead of the raw data from the source domain, however, it may leak the raw data through generative adversarial training. This paper studies a practical and interesting setting for UDA, where only a black-box source model (i.e., only network predictions are available) is provided during adaptation in the target domain. Besides, different neural networks are even allowed to be employed for different domains. For this new problem, we propose a novel two-step adaptation framework called *Distill and Fine-tune* (*Dis-tune*). Specifically, *Dis-tune* first structurally distills the knowledge from the source model to a customized target model, then unsupervisedly fine-tunes the distilled model to fit the target domain. To verify the effectiveness, we consider two UDA scenarios (i.e., closed-set and partial-set), and discover that *Dis-tune* achieves highly competitive performance to state-of-the-art approaches.

## 1. Introduction

Deep neural networks achieve remarkable progress with massive labeled data, however, it sounds expensive and not efficient to collect enough labeled data for each new task. To alleviate the burden of labeling, considerable attention has been devoted to the transfer learning field [47, 71], especially for unsupervised domain adaptation (UDA) [2, 9], where one or multiple related but different labeled datasets are collected as source domain(s) to help recognize unlabeled instances in the new dataset (called target domain). Recently, UDA methods have been widely applied in a va-

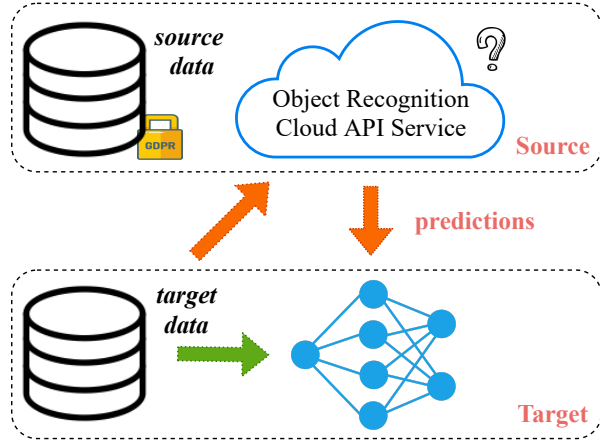


Figure 1. A challenging but interesting domain adaptation scenario where the source agent only provides a black-box model (e.g., via the cloud API service) to the target user, where neither the raw source data nor the source model is accessible during adaptation.

riety of computer vision problems, e.g., image classification [15, 61, 42], semantic segmentation [69, 60, 22], and object detection [7, 29, 51].

Existing UDA methods always require to access the raw source data and resort to domain adversarial training [61, 15] or maximum mean discrepancy minimization [62, 41] to align source features with target features. However, in many situations like personal medical records, the raw source data may be missing or should not be shared due to the privacy policy. To tackle this issue, several recent studies [38, 35, 32] attempt to utilize the trained model instead of the raw data from the source domain as supervision and obtain surprisingly good adaptation results. Nevertheless, these methods always require source models to be elegantly trained and provided to the target domain with all the details, which could raise two important concerns. First, through generation techniques like generative adversarial training [18], it is still possible to recover the raw source data, which may leak the individual information. Second, the target domain utilizes the same neural network as the source domain, which is not desirable for low-resource tar-

get users. In this paper, we study a realistic and challenging scenario for UDA, where the source model is simply trained and provided to the target domain as a black-box model.

For a better illustration, as shown in Fig. 1, the target user exploits the API service offered by the source vendor to acquire the predictions for each instance and utilizes them for adaptation in the unlabeled target domain. To address such a realistic UDA problem, we propose a novel adaptation framework called Distill and Fine-tune (Dis-tune). Briefly, Dis-tune first distills the knowledge from predictions by the source model and then fine-tunes the distilled model with the target domain itself, forming a simple two-step approach. While vanilla knowledge distillation [20] could learn the target model (student) by imitating the outputs of the source model (teacher), the distilled model is sub-optimal since the teacher performs badly in the target domain due to the domain shift. By contrast, Dis-tune acquires much better predictions from the noisy teacher outputs by considering only the highest soft-max probability and its associated class. Specifically, for each soft-max output, we only keep the largest soft-max probability and force the rest with the same values, which actually sounds like instance-specific label smoothing [70].

To leverage the structural information, we employ interpolation consistency training (ICT) [64] and mutual information maximization (IM) [38, 23] to help enhance the distillation performance. The IM objective could help increase the diversity among the target predictions which prevents noisy predictions from being biased to some easy classes to some degree. Finally, since the original teacher model performs badly due to the domain shift, we maintain an exponential moving average (EMA) prediction as a better teacher during the distillation process. Once we learn the distilled target model from the source model, it is desirable to fine-tune it using the target data alone to fit the target structure. In particular, we again employ the IM objective to fine-tune the final target model. We conduct extensive experiments on multiple UDA benchmarks and provide ablation studies to analyze the contributions of each component in our framework. Generally, the experimental results have verified the superiority of our framework.

Our main contributions can be summarized as follows:

- We study a realistic and challenging UDA scenario and propose a new adaptation framework with only a black-box model provided from the source domain.
- We propose a novel structural knowledge distillation method for UDA that merely requires the largest probability from the noisy source network predictions.
- Experiments on various UDA tasks demonstrate the superiority of the proposed Dis-tune framework over baselines. Provided with strong source models like

ViT [12], Dis-tune even achieves state-of-the-art performance for closed-set and partial-set UDA.

## 2. Related Work

**Domain Adaptation.** Domain adaptation uses labeled data in one or more source domains to solve new tasks in a target domain. In this paper, we mainly focus on a challenging problem – unsupervised domain adaptation (UDA), where no labeled data is available in the target domain. At early times, researchers address this problem via instance weighting [24, 55], feature transformation [46, 46, 36], feature space [17, 14, 56]. In the last decade, benefiting from representation learning, deep domain adaptation methods are prevailing and achieve remarkable progress. To mitigate the gap between features across different domains, domain adversarial learning [15, 61, 42, 21] and discrepancy minimization [62, 43, 31, 28] are widely used in deep UDA methods. Besides, another line of UDA methods [52, 5, 11, 26] focus on the network outputs and develop various regularization terms to pursue implicit domain alignment. In addition, researchers investigate other aspects of neural networks for UDA, *e.g.*, domain-specific normalization-based methods [45, 4] and feature regularization-based methods [65, 6]. To fully verify the effectiveness of our method, we study two different UDA settings, *i.e.*, closed-set UDA, partial-set UDA [3, 40].

**Model Transfer.** Early parameter adaptation methods [27, 13] aim to adapt the classifier trained in the source domain to the target domain with a small set of labeled examples, hence they can only be applied in the semi-supervised DA scenario. Besides empirical success, [33] pioneer the theoretical analysis of hypothesis transfer learning for linear regression. Inspired by this paradigm and increasingly important privacy concerns, [8, 37] develop several UDA methods in the absence of source data. Several recent studies [38, 32, 35] introduce this interesting setting for deep UDA, where the source domain merely offers a trained model. Specifically, [38] freezes the final classifier layer and fine-tunes the feature module via information maximization and self-supervised pseudo-labeling in the target domain. [35] leverages a conditional generative adversarial net and incorporates generated images into the adaptation process. [32] also introduces a generator and explores conditional entropy for universal domain adaptation. However, exposing details of the trained source model is risky due to some committed white-box attacks. Faced with a black-box source model, [39] divide the target dataset into two splits according to the uncertainty of their predictions, then employ a popular semi-supervised algorithm to enhance the performance of the uncertain split. Moreover, [68] proposes an iterative noisy label learning approach and [50] develops a differentiable transformation network to bring target data closer to the source domain.

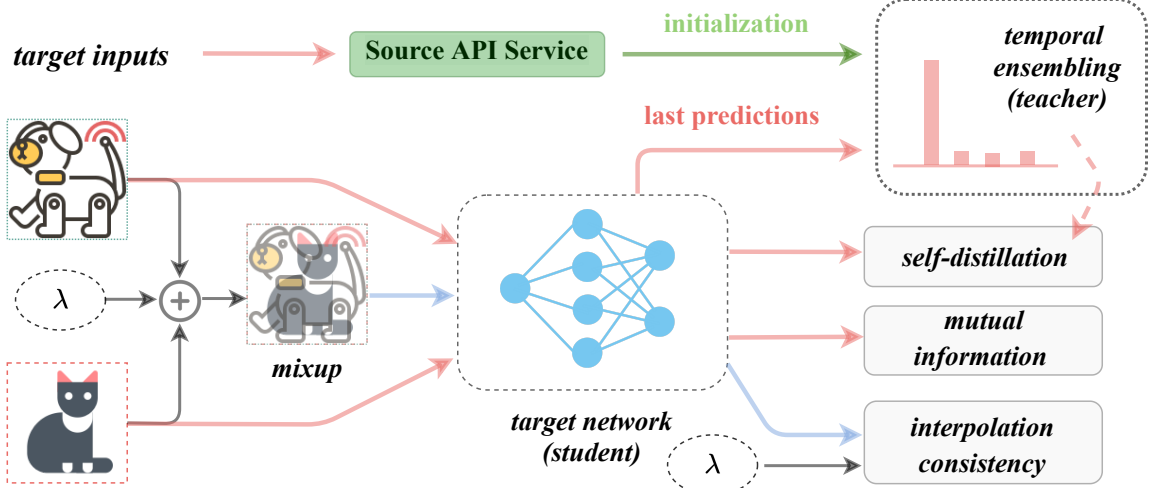


Figure 2. An overview of the proposed framework. Here the black-box source model (*i.e.*, API service) is merely required to initialize the memory bank that stores the predictions of each target instance. During the distillation step, the memory bank could be considered as a teacher that maintains an exponential moving average (EMA) prediction. In fact, three objectives describe the point-wise, batch-wise, and pair-wise information, respectively. During the fine-tuning step, only the mutual information objective is activated.

**Knowledge Distillation.** Knowledge distillation aims to transfer knowledge from one model (*i.e.*, teacher) to another model (*i.e.*, student), usually from a larger one to a smaller one. [20] shows that augmenting the training of student with a distillation loss that matches the predictions between teacher and student is beneficial. In fact, knowledge distillation could be considered as a learned label smoothing regularization [57], which has a similar function with the latter [66]. Recently, [30] proposes self-knowledge distillation and shows that, even within the same neural network, the past predictions could be the teacher itself. Besides supervised training, such self-distillation could be effectively applied with unlabeled data for semi-supervised learning. For instance, [34] proposes to ensemble predictions during training, using the outputs of a single network on different training epochs, as a teacher for the current epoch. Instead of maintaining an exponential moving average (EMA) prediction in [34], [59] utilizes an average of consecutive student models (past model weights) as a stronger teacher.

### 3. Method

We aim to address an interesting, realistic but challenging UDA setting where only one black-box source model is provided to the target domain. In this paper, we mainly focus on the  $K$ -way cross-domain image classification task. For a vanilla closed-set UDA problem, the source domain  $\{x_s^i, y_s^i\}_{i=1}^{n_s}$  consists of  $n_s$  labeled instances, where  $x_s^i \in \mathcal{X}_s, y_s^i \in \mathcal{Y}_s$ , and the target domain  $\{x_t^i, y_t^i\}_{i=1}^{n_t}$  consists of  $n_t$  unlabeled instances, where  $x_t^i \in \mathcal{X}_t, y_t^i \in \mathcal{Y}_t$ , and the goal of UDA is to infer the values of  $\{y_t^i\}_{i=1}^{n_t}$ . For closed-set UDA,  $\mathcal{Y}_s = \mathcal{Y}_t$ , namely, the label space is the same across

domains. For partial-set UDA [3],  $\mathcal{Y}_s \supset \mathcal{Y}_t$ , namely, some source classes does not exist in the target domain. Concerning the black-box adaptation setting here, only one trained source model is provided, without requiring access to the source data. Note that, different from prior model adaptation methods [38, 35], we also require no details about the source model, *e.g.*, backbone type and network parameters. Instead, only *the network predictions of the target instances  $\mathcal{X}_t$  from the source model  $f_s : \mathcal{X}_s \rightarrow \mathcal{Y}_s$*  are utilized for adaptation in the target domain.

### 3.1. Architecture and Source Model Generation

We first describe how to obtain the trained model from the source domain in the following. Unlike [38] that elegantly designs the source model with a bottleneck layer and the weight normalization [53] technique, we simply employ a single linear fully-connected (FC) layer after the backbone feature network, and employ the widely-used label smoothing [57] technique to train  $f_s$  below,

$$\mathcal{L}_s(f_s; \mathcal{X}_s, \mathcal{Y}_s) = -\mathbb{E}_{(x_s, y_s) \in \mathcal{X}_s \times \mathcal{Y}_s} (q^s)^T \log f_s(x_s), \quad (1)$$

where  $q^s = (1 - \alpha)\mathbf{1}_{y_s} + \alpha/K$  is the smoothed label vector and  $\alpha$  is the smoothing parameter empirically set to 0.1, where  $\mathbf{1}_j$  denotes a  $K$ -dimensional one-hot vector with only the  $j$ -th value being 1.

As for the self-defined target network  $f_t : \mathcal{X}_t \rightarrow \mathcal{Y}_t$ , we follow [38] and adopt the bottleneck layer consisting of a batch-normalization layer and a FC layer, and the classifier consisting of a weight-normalization layer and a FC layer.

### 3.2. Noisy Knowledge Distillation

In order to extract knowledge from a black-box model, there exists a natural solution called knowledge distillation (KD) [20] by forcing the target model (student) to learn similar predictions to the source model (teacher). However, existing KD methods are applied to a supervised training task, and the consistency loss in the following works well by acting as a regularization term,

$$\mathcal{L}_{kd}(f_t; \mathcal{X}_t, f_s) = \mathbb{E}_{x_t \in \mathcal{X}_t} \mathcal{D}_{kl}(f_s(x_t) \parallel f_t(x_t)), \quad (2)$$

where  $\mathcal{D}_{kl}$  denotes the Kullback-Leibler (KL) divergence loss. However, for the studied black-box adaptation problem here, the network outputs from the source model  $f_s$  for target instances are not accurate and noisy, and highly relying on the teacher  $f_s(x_t)$  via a consistency loss above sounds not desirable any more. To address this issue, we revise the teacher output via the largest value and propose a new distillation objective in the following,

$$\mathcal{L}_{kd}^{top}(f_t; \mathcal{X}_t, f_s) = \mathbb{E}_{x_t \in \mathcal{X}_t} \mathcal{D}_{kl}(g(f_s(x_t)) \parallel f_t(x_t)),$$

$$g_i(p) = \begin{cases} \max_j p_j & i = \arg \max_j p_j, \\ (1 - \max_j p_j)/(K - 1) & \text{otherwise,} \end{cases} \quad (3)$$

where only the index corresponding to the largest probabilistic score is remained. The refined output  $g(f_s(x_t))$  is believed to work better than the original output  $f_s(x_t)$  for several reasons below, 1) it partially neglects some redundant and noisy information by only focusing on the pseudo label (class associated with the largest value) and forcing a uniform distribution on other classes like label smoothing [57]; 2) it does not solely rely on the noisy pseudo label but utilizes the largest value as confidence, similar to self-weighted pseudo labeling [25]. As a byproduct, using the smoothed output means that we *do not even need the full K-dimensional soft-max vector but the predicted class along with its maximum probability*, which sounds more flexible when using an API service provided by other companies.

### 3.3. Structural Knowledge Distillation

As stated above, the teacher output from the source model is highly possible to be inaccurate and noisy due to the domain shift. Even we propose a much better solution in Eq. (3), only the point-wise information is considered during the distillation process, it ignores the data structure in the target domain, thus is not enough for effective noisy knowledge distillation. As such, we incorporate the structural information in the target domain to regularize the distillation. First, we consider the pairwise structural information via MixUp [67], and employ the interpolation consistency training (ICT) [64] technique as below,

$$\mathcal{L}_{ict}(f_t; \mathcal{X}_t) = \mathbb{E}_{x_i^t, x_j^t \in \mathcal{X}_t} \mathbb{E}_{\lambda \in \text{Beta}(\alpha, \alpha)} l_{ce}(\text{Mix}_{\lambda}(f_t(x_i^t), f_t(x_j^t)), f_t(\text{Mix}_{\lambda}(x_i^t, x_j^t))), \quad (4)$$

where  $\text{Mix}_{\lambda}(a, b) = \lambda \cdot a + (1 - \lambda) \cdot b$  denotes the MixUp operation, and  $\lambda$  is sampled from a Beta distribution, and  $\alpha$  is the hyper-parameter empirically set to 0.3.  $f_t'$  just offers the values of  $f_t$  but needs no gradient optimization. Here we do not adopt the EMA update strategy in [64] for  $f_t'$ . The ICT objective in Eq. (4) can be considered to augment the target domain with more interpolated samples, which is beneficial for better generalization ability.

In addition, we also consider the global structural information during distillation in the target domain. In fact, during distillation, the classes with a large number of instances are relatively easy to learn, which may wrongly recognize some confusing target instances as such classes in turn. To circumvent this problem, we attempt to encourage the diversity among the predictions of all the target instance. Specifically, we try to maximize the widely-used mutual information objective [16, 23, 38] in the following,

$$\begin{aligned} \mathcal{L}_{mi}(f_t; \mathcal{X}_t) &= H(\mathcal{Y}_t) - H(\mathcal{Y}_t | \mathcal{X}_t) \\ &= h(\mathbb{E}_{x_t \in \mathcal{X}_t} f_t(x_t)) - \mathbb{E}_{x_t \in \mathcal{X}_t} h(f_t(x_t)), \end{aligned} \quad (5)$$

where  $h(p) = -\sum_i p_i \log p_i$  denotes the conditional entropy function. Obviously, increasing the marginal entropy  $H(\mathcal{Y}_t)$  encourages the label distribution to be uniform, while decreasing the conditional entropy  $H(\mathcal{Y}_t | \mathcal{X}_t)$  encourages unambiguous network predictions.

While combining three objectives in Eq. (3), Eq. (4), and Eq. (5) introduced above, the overall optimization objective can be written as

$$\mathcal{L}_t = \mathcal{L}_{kd}^{top} + \beta \mathcal{L}_{ict} - \mathcal{L}_{mi}, \quad (6)$$

where  $\beta > 0$  is a hyper-parameter controlling the importance of the ICT objective during structural distillation.

Different from the most closely related work [68] that iteratively refines the pseudo labels and learns the classification network, our framework directly learns good network predictions for the target data as a unified approach, which is more desirable to capture the data structure of the target domain.

To further alleviate the noisy outputs from the original source model, we follow Temporal Ensembling [34] and develop a self-distillation strategy, shown in Fig. 2. In particular, it maintains an EMA prediction by

$$f_s(x_t) \leftarrow \gamma f_s(x_t) + (1 - \gamma) f_t(x_t), \quad \forall x_t \in \mathcal{X}_t, \quad (7)$$

where  $\gamma$  is a momentum hyper-parameter, and  $f_s(x_t)$  is initialized by the source model. Following [34], we update the prediction after every training epoch. When  $\gamma = 1$ , there exists no temporal ensembling, namely, the source model always acts as a teacher during distillation.

### 3.4. Fine-tuning the Distilled Model

Through the proposed structural knowledge distillation method from the black-box source model  $f_s$ , it is ex-

pected to learn a well-performing white-box target model. However, the distilled model seems sub-optimal since it is mainly optimized via the point-wise knowledge distillation term in Eq. (3), which highly depends on the source model. Inspired by [54], we hypothesize that a better network is achievable by introducing a secondary training phase that solely minimizes the target-side cluster assumption violation. Rather than employ the parameter-sensitive virtual adversarial training [54], we again adopt the mutual information in Eq. (5) to refine the distilled target model.

So far, we have shown all the details of two steps within the proposed framework (Dis-tune). Besides, we also provide a full description in Algorithm 1 for Dis-tune.

#### Algorithm 1 Pseudocode of Dis-tune for black-box UDA.

##### 1. Source model generation:

**Require:**  $\{x_s^i, y_s^i\}_{i=1}^{n_s}$ , the number of epochs  $T_m$ .  
▷ Train  $f_s$  via minimizing the objective in Eq. (1).

##### 2. Distillation:

**Require:** Target data  $\{x_t^i\}_{i=1}^{n_t}$ ,  $T_m$ , parameters  $\alpha, \beta, \gamma$ .  
for  $e = 1$  to  $T_m$  do  
    for  $i = 1$  to  $n_b$  do

        ▷ Sample a batch from target data.  
        ▷ Apply MixUp within the batch.  
        ▷ Update  $f_t$  via minimizing the objective in Eq. (6).

    end for

    ▷ Update the teacher output  $f_s(x_t)$  via Eq. (7).

end for

##### 3. Fine-tuning:

**Require:** Target data  $\{x_t^i\}_{i=1}^{n_t}$ ,  $T_m$ ,  $m$ .  
▷ Fine-tune  $f_t$  via maximizing the objective in Eq. (5).

## 4. Experiments

### 4.1. Setup

**Datasets.** Digits is a widely-used benchmark in the UDA literature. We follow the protocol of [21, 42, 38] and focus on three UDA tasks, *i.e.*, SVHN→MNIST, USPS→MNIST, and MNIST→USPS. For each task, we utilize all the samples in the training splits of each domain during training and report the results on the test split of the target domain.

**Office** [49] is a popular benchmark on cross-domain object recognition, consisting of three different domains in 31 categories, *i.e.*, Amazon (**A**), DSLR (**D**), and Webcam (**W**).

**Office-Home** [63] is a challenging medium-sized benchmark on object recognition, consisting of four different domains in 65 categories, *i.e.*, Artistic images (**Ar**), Clip Art (**Cl**), Product images (**Pr**), and Real-World images (**Rw**).

**VisDA-C** [48] is a large-scale benchmark developed for 12-class synthetic-to-real object recognition. The source domain contains 152 thousand synthetic images generated by rendering 3D models while the target domain has 55 thousand real object images sampled from Microsoft COCO.

Table 1. Accuracies (%) on Digits for UDA. (Best in **bold**)

Methods	S → M	U → M	M → U	Avg.
Source-only	71.6±1.1	92.5±0.3	90.4±0.8	84.9
NLL-OT	93.7±1.8	96.4±0.2	85.0±0.5	91.7
NLL-KL	94.3±1.3	96.6±0.5	92.9±0.4	94.6
SHOT-ST	98.2±0.2	<b>97.6</b> ±0.7	94.6±0.1	96.8
SHOT-WST	98.3±0.1	97.3±0.5	87.4±0.1	94.3
Dis- (ours)	97.5±0.4	96.5±0.6	94.2±0.2	96.1
Dis-tune (ours)	<b>98.5</b> ±0.1	97.3±0.1	<b>95.2</b> ±0.3	<b>97.0</b>
SHOT [38]	98.9±0.0	98.4±0.6	98.0±0.2	98.4
SHOT++ [39]	98.9±0.1	98.5±0.8	98.5±0.1	98.6
CyCADA [21]	90.4±0.4	96.5±0.1	95.6±0.4	94.2
STAR [44]	98.8±0.1	97.7±0.1	97.8±0.1	98.1

Table 2. Accuracies (%) on Office for closed-set UDA.

Method	A → D	A → W	D → A	D → W	W → A	W → D	Avg.
<b>ResNet-50</b> (source backbone) → <b>ResNet-50</b> (target backbone)							
Source-only	79.2	76.3	59.3	94.1	61.2	98.6	78.1
NLL-OT	88.8	86.8	66.6	94.5	67.3	95.4	83.2
NLL-KL	89.1	86.8	66.2	96.9	67.3	97.9	84.0
SHOT-ST	84.9	82.3	66.9	95.7	68.2	98.3	82.7
SHOT-WST	89.0	83.9	69.8	96.0	70.5	97.6	84.5
Dis- (ours)	89.5	85.1	71.1	97.3	71.4	98.6	85.5
Dis-tune (ours)	91.0	85.1	72.4	98.1	73.1	98.7	86.4
<b>ResNet-101</b> (source backbone) → <b>ResNet-50</b> (target backbone)							
Source-only	82.3	81.0	58.3	95.3	64.9	98.7	80.1
NLL-OT	89.9	90.7	68.4	94.2	70.7	95.4	84.9
NLL-KL	90.5	90.6	68.7	96.5	70.5	98.0	85.8
SHOT-ST	90.6	88.8	69.9	96.5	71.1	98.5	85.9
SHOT-WST	92.0	89.6	71.9	97.7	72.9	98.1	87.0
Dis- (ours)	92.2	89.3	72.7	98.8	74.2	98.7	87.7
Dis-tune (ours)	93.4	89.6	73.6	98.9	75.4	99.1	88.3
<b>ViT</b> (source backbone) → <b>ResNet-50</b> (target backbone)							
Source-only	88.0	89.8	74.8	97.7	77.7	99.8	88.0
NLL-OT	90.8	91.1	76.0	93.7	77.9	94.6	87.4
NLL-KL	<b>92.1</b>	93.4	77.3	97.8	79.3	99.5	89.9
SHOT-ST	88.9	90.8	75.4	98.1	78.2	99.8	88.5
SHOT-WST	91.4	92.2	76.9	98.9	79.3	99.9	89.8
Dis- (ours)	91.9	95.0	80.1	<b>99.0</b>	81.5	<b>99.9</b>	91.2
Dis-tune (ours)	92.0	<b>95.2</b>	<b>80.2</b>	<b>99.0</b>	<b>81.6</b>	<b>99.9</b>	<b>91.3</b>
Model-dependent and Data-dependent UDA Methods via <b>ResNet-50</b>							
SHOT [38]	94.0	90.1	74.7	98.4	74.3	99.9	88.6
SHOT++ [39]	94.5	90.9	76.3	98.6	75.8	99.9	89.3
CAN [28]	95.0	94.5	78.0	99.1	77.0	99.8	90.6
SRDC [58]	95.8	95.7	76.7	99.2	77.1	100.	90.8

**Implementation<sup>1</sup> details.** Generally, we randomly run our methods for three times with different random seeds {2019, 2020, 2021} via **PyTorch** and report the average accuracies. Regarding the source model  $f_s$ , we train it using all the samples in the source domain. In this paper, we consider three different backbones, ResNet-50 [19], ResNet-101 [19], and

<sup>1</sup><https://github.com/tim-learn/Dis-tune/>.

Table 3. Accuracies (%) on Office-Home for closed-set UDA.

Method	Ar→Cl	Ar→Pr	Ar→Re	Cl→Ar	Cl→Pr	Cl→Re	Pr→Ar	Pr→Cl	Pr→Re	Re→Ar	Re→Cl	Re→Pr	Avg.
<b>ResNet-50</b> (source backbone) → <b>ResNet-50</b> (target backbone)													
Source-only	44.3	67.3	74.8	54.7	63.6	66.4	52.7	41.0	73.2	65.7	46.6	78.0	60.7
NLL-OT	49.0	70.2	76.6	57.0	67.7	71.9	54.8	46.1	75.5	63.8	52.1	77.6	63.5
NLL-KL	49.8	71.6	77.4	58.7	68.6	72.6	56.1	46.0	76.8	65.8	52.1	79.8	64.6
SHOT-ST	48.9	73.5	77.5	60.4	69.7	73.0	56.8	46.5	76.3	67.2	52.9	80.3	65.3
SHOT-WST	50.4	75.8	78.8	63.6	72.4	76.2	60.1	47.1	79.1	69.1	54.4	81.7	67.4
Dis- (ours)	50.5	77.2	80.2	64.0	75.1	76.7	60.7	47.6	80.5	69.1	54.1	83.1	68.2
Dis-tune (ours)	52.9	78.3	81.5	65.3	76.1	77.8	62.4	50.3	81.8	70.5	55.9	84.1	69.7
<b>ResNet-101</b> (source backbone) → <b>ResNet-50</b> (target backbone)													
Source-only	49.5	70.1	77.4	57.0	67.2	68.5	55.2	44.1	75.1	68.4	49.6	79.8	63.5
NLL-OT	55.2	73.7	78.9	60.9	72.0	75.4	59.2	49.7	77.3	66.7	56.2	80.1	67.1
NLL-KL	55.6	75.4	80.3	63.1	73.6	76.1	60.8	49.7	78.9	69.2	56.7	82.6	68.5
SHOT-ST	54.3	75.6	80.5	62.7	74.8	75.6	61.9	49.9	78.9	70.3	55.2	82.9	68.6
SHOT-WST	54.8	77.7	81.6	65.6	76.7	78.0	63.5	51.7	81.1	71.4	56.6	84.0	70.2
Dis- (ours)	55.5	79.3	82.4	64.3	78.1	78.6	63.8	51.8	81.5	71.4	56.8	85.0	70.7
Dis-tune (ours)	56.7	80.2	83.6	65.3	80.0	79.6	64.7	53.6	82.7	72.0	58.5	85.7	71.9
<b>ViT</b> (source backbone) → <b>ResNet-50</b> (target backbone)													
Source-only	55.0	83.4	87.6	77.5	83.7	86.2	75.0	50.6	87.4	78.9	53.2	86.7	75.4
NLL-OT	58.9	80.2	84.9	71.0	81.1	83.8	69.7	54.5	84.8	72.6	57.8	82.8	73.5
NLL-KL	60.1	85.4	88.1	77.3	85.3	86.8	75.2	55.9	87.9	78.2	58.9	87.7	77.2
SHOT-ST	57.5	84.4	87.6	77.9	84.8	86.2	75.6	56.8	87.4	79.1	57.1	87.2	76.8
SHOT-WST	59.3	85.5	88.3	79.0	86.6	86.8	76.8	57.6	88.2	80.7	58.9	87.9	78.0
Dis- (ours)	61.5	85.4	86.0	80.6	89.1	87.9	79.0	61.1	89.2	81.7	63.8	89.3	79.5
Dis-tune (ours)	61.8	85.4	86.2	80.7	89.5	87.9	79.1	62.4	89.2	81.8	64.5	89.6	79.9
Model-dependent and Data-dependent UDA Methods via <b>ResNet-50</b>													
SHOT [38]	57.1	78.1	81.5	68.0	78.2	78.1	67.4	54.9	82.2	73.3	58.8	84.3	71.8
SHOT++ [39]	58.1	79.5	82.4	68.6	79.9	79.3	68.6	57.2	83.0	74.3	60.4	85.1	73.0
HDAN [10]	56.8	75.2	79.8	65.1	73.9	75.2	66.3	56.7	81.8	75.4	59.7	84.7	70.9
SRDC [58]	52.3	76.3	81.0	69.5	76.2	78.0	68.7	53.8	81.7	76.3	57.1	85.0	71.3

ViT-B\_16 [12] (ViT for simplicity). Following [38], mini-batch SGD is employed to learn the layers initialized from the ImageNet pre-trained model or last stage with the learning rate (1e-3), and new layers from scratch with the learning rate (1e-2). Besides, we use the suggested training settings in [42, 38], including learning rate scheduler, momentum (0.9), weight decay (1e-3), bottleneck size (256), and batch size (64). Concerning the parameters in Dis-tune,  $T_m = 30$  is adopted for all datasets except  $T_m = 10$  for **VisDA-C**. Moreover,  $\alpha = 0.3$  is fixed for all UDA tasks, and  $\beta = 1.0, \gamma = 0.6$  is utilized for object recognition and  $\beta = 0.1, \gamma = 0.6$  is utilized for digit classification.

**Baselines.** Since the black-box UDA setting is fairly new in this field, we come up with several baseline methods below,

- **NLL-KL** mainly follows the idea of noisy label learning (NLL) [68] and adopts the diversity-promoting KL divergence to refine the noisy pseudo labels, then train a network with the refined pseudo labels iteratively.
- **NLL-OT** differs from NLL-KL only in that the optimal transport (OT) technique [1] is employed instead of the KL divergence in the refining step.
- **SHOT-ST** first learns a white-box model by self-training (ST) in the target domain and then exploits SHOT [38]

for further adaptation. ST treats the class predicted by  $f_s$  as the true label for each target instance and employs a cross-entropy loss to train the model.

- **SHOT-WST** differs from SHOT-ST only in that a weighted cross-entropy loss is utilized where the predictive confidence is treated as the instance weight.

Regarding our methods, we provide Dis- (w/o the second fine-tuning step in Algorithm 1) in addition to the two-step Dis-tune. For model-dependent (model transfer) UDA methods, we choose state-of-the methods, *i.e.*, SHOT [38] and SHOT++ [39]. For traditional data-dependent UDA methods, to the best of our knowledge, we display the best-performing results for different datasets.

## 4.2. Results

As shown in Table 1, we compare our methods against source-only and four baselines for **Digits**. All the black-box UDA methods beat the source-only method, and SHOT-ST achieves the best mean accuracy. Dis-tune achieves the best results in 2 out of 3 tasks and performs better than other baselines including SHOT-ST. Compared with model-/data-dependent methods, Dis-tune even outperforms CyCADA [21] and achieves competitive results to them.

Table 4. Accuracies (%) on VisDA-C for closed-set UDA.

Method	plane	bcycl	bus	car	horse	knife	mcycle	person	plant	sktbrd	train	truck	Per-class
<b>ResNet-50</b> (source backbone) → <b>ResNet-50</b> (target backbone)													
Source-only	68.4	12.5	50.8	60.8	55.0	2.1	77.5	25.1	60.7	21.3	87.7	5.0	43.9
NLL-OT	95.4	81.0	74.4	42.5	91.1	13.5	74.7	65.4	84.5	69.0	79.4	44.5	68.0
NLL-KL	94.7	79.9	75.1	46.0	90.4	14.4	75.5	67.4	83.7	71.7	78.7	45.2	68.6
SHOT-ST	94.1	81.3	74.5	46.4	90.2	16.8	67.1	76.6	82.7	83.1	75.1	59.8	70.6
SHOT-WST	94.2	82.3	75.0	47.7	90.3	16.6	67.9	76.2	82.8	83.0	74.9	59.4	70.9
Dis- (ours)	94.8	68.0	76.5	70.7	93.0	1.0	88.4	79.8	90.4	72.7	87.7	10.1	69.4
Dis-tune (ours)	94.0	84.8	77.0	55.9	91.8	9.6	76.4	80.4	89.2	81.8	86.5	17.3	70.4
<b>ResNet-101</b> (source backbone) → <b>ResNet-50</b> (target backbone)													
Source-only	68.8	22.1	50.7	74.7	68.9	12.7	81.3	31.0	65.3	26.9	80.9	8.7	49.3
NLL-OT	80.8	81.7	74.9	41.7	91.3	33.8	74.7	70.8	85.2	74.9	82.3	47.3	70.0
NLL-KL	78.6	81.8	76.0	45.4	91.1	33.1	77.1	73.2	84.7	76.7	82.2	48.7	70.7
SHOT-ST	58.5	85.2	74.6	42.9	90.4	33.2	70.5	79.9	88.3	84.1	80.2	60.7	70.7
SHOT-WST	60.3	85.1	72.9	42.9	89.3	32.8	70.0	79.0	87.8	84.5	78.7	59.5	70.2
Dis- (ours)	68.0	74.0	76.9	74.4	92.7	32.0	88.9	83.6	89.6	85.4	84.3	21.3	72.6
Dis-tune (ours)	81.2	85.6	75.7	55.5	91.1	35.0	76.5	80.1	89.5	86.8	83.9	35.5	73.0
<b>ViT</b> (source backbone) → <b>ResNet-50</b> (target backbone)													
Source-only	96.1	52.8	80.2	78.3	91.6	55.4	91.2	12.8	79.4	89.4	95.8	15.0	69.8
NLL-OT	97.9	89.9	78.9	43.6	93.7	93.5	77.8	43.9	91.9	95.7	90.0	52.5	79.1
NLL-KL	97.0	88.3	81.0	50.5	94.8	95.0	84.0	50.9	90.3	95.3	90.0	53.6	80.9
SHOT-ST	96.0	90.0	81.0	44.8	94.9	97.4	80.9	72.0	93.3	91.0	88.2	70.0	83.3
SHOT-WST	95.6	89.3	79.1	42.4	93.1	97.6	79.6	65.8	92.0	88.0	87.5	68.1	81.5
Dis- (ours)	96.7	82.3	83.1	77.2	95.1	96.9	93.1	75.9	94.2	94.9	92.8	45.0	85.6
Dis-tune (ours)	95.2	89.5	81.6	58.4	93.5	95.9	81.7	75.7	93.1	93.5	90.1	57.5	83.8
Model-dependent and Data-dependent UDA Methods via <b>ResNet-101</b>													
SHOT [38]	94.3	88.5	80.1	57.3	93.1	94.9	80.7	80.3	91.5	89.1	86.3	58.2	82.9
SHOT++ [39]	95.8	88.3	90.5	84.7	97.9	98.0	92.9	85.3	97.5	92.9	93.9	32.3	87.5
STAR [44]	95.0	84.0	84.6	73.0	91.6	91.8	85.9	78.4	94.4	84.7	87.0	42.2	82.7
CAN [28]	97.0	87.2	82.5	74.3	97.8	96.2	90.8	80.7	96.6	96.3	87.5	59.9	87.2

We show the results of cross-domain object recognition on **Office-Home** in Table 3. As stated above, we adopt three different backbone networks for training the source domain. Typically, UDA methods assume the same network structure across domains, *e.g.*, ResNet-50 in [42, 10, 58]. With the same ResNet-50 backbone, Dis-tune performs better than Dis- and other baselines, indicating the effectiveness of the proposed distillation strategy and the following fine-tuning step. In fact, the mean accuracy of Dis-tune even approaches that of HDAN [10], one of the state-of-the-art data-dependent methods. With much stronger source models with better source-only results, all the black-box UDA methods are clearly strengthened, and Dis-tune achieves the best mean accuracy 80.5% with ViT.

As can be seen from Table 4, the results on **VisDA-C** again validate the superiority of our Dis- and Dis-tune over baselines. Similar observations are discovered on this dataset, namely, the stronger the source model is, the better results black-box UDA methods obtain, and the proposed Dis-tune slightly outperforms Dis-. Typically, UDA meth-

ods always assume the same network structure (ResNet-101) across domains. Compared with these methods, the proposed method Dis-tune obtains a competitive result with the ResNet-50 backbone used in the target domain.

In addition to the closed-set UDA problem, we also investigate the generalization ability of these black-box methods for partial-set UDA. We follow [3, 40] and only select the first 25 classes in alphabetical order in the target domain. As shown in Table 5, NLL-OT and NLL-KL even under-perform the source-only method due to the challenging asymmetric label spaces. Moreover, our Dis- and Dis-tune achieve better results than SHOT-ST and SHOT-WST. Different from previous tables, here the second fine-tuning step does not work well since simply promoting the diversity is not encourage for partial-set UDA. With the ViT-based source model, Dis- obtains the highest mean accuracy (81.5%) which is also fairly higher than previous state-of-the-art results in [39] via ResNet-50.

Generally, our methods (including the distillation and fine-tuning strategies) work well for black-box UDA.

Table 5. Accuracies (%) on Office-Home for partial-set UDA.

Method	Ar→Cl	Ar→Pr	Ar→Re	Cl→Ar	Cl→Pr	Cl→Re	Pr→Ar	Pr→Cl	Pr→Re	Re→Ar	Re→Cl	Re→Pr	Avg.
<b>ResNet-50 (source backbone) → ResNet-50 (target backbone)</b>													
Source-only	44.7	70.4	80.8	56.6	61.7	67.0	60.6	40.5	76.2	70.9	48.5	77.5	63.0
NLL-OT	36.2	45.8	51.6	45.0	44.4	48.4	44.3	35.3	49.6	49.3	38.7	49.4	44.8
NLL-KL	39.6	52.4	59.1	49.4	49.7	55.4	49.3	37.9	57.8	55.3	42.2	57.7	50.5
SHOT-ST	52.9	76.9	85.4	67.0	70.4	78.4	68.2	49.3	81.8	76.8	54.7	81.1	70.2
SHOT-WST	55.4	81.5	89.0	73.5	75.1	81.8	71.2	50.8	84.6	80.6	59.6	84.3	74.0
Dis- (ours)	56.7	84.2	90.3	77.1	79.8	81.9	72.3	56.4	86.4	80.8	62.3	85.7	76.2
Dis-tune (ours)	57.7	84.5	90.3	78.5	81.0	81.9	73.8	57.7	87.3	81.7	63.2	85.6	76.9
<b>ResNet-101 (source backbone) → ResNet-50 (target backbone)</b>													
Source-only	51.9	71.9	82.3	59.6	62.7	69.0	61.2	45.7	77.4	72.4	50.4	78.5	65.3
NLL-OT	40.8	47.1	53.0	46.4	45.6	49.5	47.1	38.1	51.1	49.6	40.2	51.1	46.6
NLL-KL	44.3	55.9	60.3	51.3	51.9	58.2	51.8	41.1	58.2	56.9	44.5	58.3	52.7
SHOT-ST	58.8	77.9	87.5	71.7	72.1	77.5	69.2	52.9	81.9	78.3	55.2	81.7	72.1
SHOT-WST	62.3	84.3	89.8	76.1	76.1	83.8	71.3	56.8	84.1	80.9	60.1	86.0	76.0
Dis- (ours)	65.9	<b>88.3</b>	<b>91.0</b>	79.2	80.4	86.0	74.5	60.4	87.6	82.2	63.9	<b>88.4</b>	79.0
Dis-tune (ours)	<b>66.6</b>	88.2	90.9	80.1	80.7	85.6	74.7	<b>61.8</b>	87.9	81.9	<b>64.5</b>	88.1	79.3
<b>ViT (source backbone) → ResNet-50 (target backbone)</b>													
Source-only	55.5	83.5	89.7	78.6	80.7	84.4	78.2	46.7	87.7	83.7	53.2	85.6	75.6
NLL-OT	37.9	44.3	45.6	44.1	45.7	44.7	44.8	34.2	45.1	45.3	36.7	45.5	42.8
NLL-KL	46.2	58.6	63.2	58.2	57.7	59.5	56.0	41.0	60.5	58.8	43.6	58.6	55.2
SHOT-ST	54.8	82.1	87.9	79.4	77.1	81.9	77.7	49.1	86.1	84.1	53.6	81.6	74.6
SHOT-WST	57.6	84.4	89.6	81.4	80.5	85.6	82.2	51.1	88.8	<b>86.3</b>	57.0	84.9	77.5
Dis- (ours)	64.1	87.9	90.5	<b>83.4</b>	<b>88.1</b>	<b>87.2</b>	<b>84.3</b>	60.6	<b>91.1</b>	86.1	63.7	87.7	<b>81.2</b>
Dis-tune (ours)	63.7	87.7	90.4	83.2	88.0	86.9	84.2	60.4	91.0	86.0	63.9	87.6	81.1
Model-dependent and Data-dependent UDA Methods via ResNet-50													
SHOT [38]	64.8	85.2	92.7	76.3	77.6	88.8	79.7	64.3	89.5	80.6	66.4	85.8	79.3
SHOT++ [39]	66.0	86.1	92.8	77.9	77.5	87.6	78.6	66.4	89.7	81.5	67.9	87.2	79.9
MCC [26]	63.1	80.8	86.0	70.8	72.1	80.1	75.0	60.8	85.9	78.6	65.2	82.8	75.1
BA <sup>3</sup> US [40]	60.6	83.2	88.4	71.8	72.8	83.4	75.5	61.6	86.5	79.3	62.8	86.1	76.0

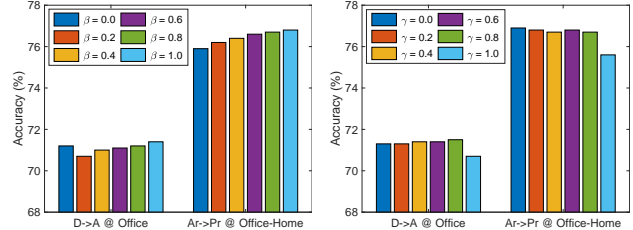
Table 6. **Ablation.** Results of different variants of Dis- (ours) for closed-set UDA with **ResNet-50** (source) → **ResNet-50** (target).

Top	$\mathcal{L}_{mi}$	$\mathcal{L}_{ict}$	EMA	Ar→Cl	Ar→Pr	Ar→Re	Avg.
×	×	×	×	45.5±0.3	69.5±0.2	75.7±0.3	63.6
✓	✓	✓	✓	47.0±0.3	71.2±0.3	76.6±0.1	64.9
✓	✓	✓	✓	47.5±0.3	71.8±0.1	77.1±0.1	65.5
✓	✓	✓	✓	50.8±0.4	74.7±0.2	78.7±0.2	68.1
✓	✓	✓	✓	<b>51.5</b> ±0.6	75.6±0.2	79.4±0.3	68.8
✓	✓	✓	✓	50.5±0.1	<b>77.2</b> ±0.1	<b>80.2</b> ±0.2	<b>69.3</b>

### 4.3. Analysis

We further study the contribution of four components within our Dis-, *i.e.*, ‘Top’ denotes the usage of  $g$  in Eq.(3), and ‘EMA’ denotes  $\gamma < 1$ , and  $\mathcal{L}_{mi}, \mathcal{L}_{ict}$  denote their existence in  $\mathcal{L}_t$ . As reported in Table 6, we provide the accuracies on three closed-set UDA tasks on **Office-Home**. It is clear to find that all these components are always effective.

Besides, we also analyze the sensitivity of parameters  $\beta, \gamma$  within Dis- for D→A and Ar→Pr in Fig. 3. Specifically,  $\beta$  is in the range of [0.0, 0.2, 0.4, 0.6, 0.8, 1.0], and  $\gamma$  is in the range of [0.0, 0.2, 0.4, 0.6, 0.8, 1.0]. As can be seen from Fig. 3(a), a larger value for  $\beta$  is always desirable, namely, the ICT objective is indeed effective during distillation. As for the moving momentum parameter, the performance around  $\gamma = 0.6$  is also stable.

(a) sensitivity of parameter  $\beta$       (b) sensitivity of parameter  $\gamma$ Figure 3. Accuracies of Dis- with different values of  $\beta, \gamma$ .

### 5. Conclusion

We explore an interesting, realistic but challenging UDA setting where the source domain only provides a black-box model to the target domain, even allowing different networks for different domains. From the perspective of knowledge distillation, we propose a simple yet effective two-step framework called Distill and Fine-tune (Dis-tune). Dis-tune elegantly refines the noisy teacher output and fully considers the data structure in the target domain during distillation and fine-tuning. Experiments on multiple datasets verify the superiority of Dis-tune over baselines for different UDA tasks. Provided with a strong pre-trained source model, our Dis-tune even achieves state-of-the-art results.

## References

- [1] YM Asano, C Rupprecht, and A Vedaldi. Self-labelling via simultaneous clustering and representation learning. In *International Conference on Learning Representations (ICLR)*, 2019. 6
- [2] Shai Ben-David, John Blitzer, Koby Crammer, Fernando Pereira, et al. Analysis of representations for domain adaptation. In *Advances in Neural Information Processing Systems (NeurIPS)*, 2007. 1
- [3] Zhangjie Cao, Lijia Ma, Mingsheng Long, and Jianmin Wang. Partial adversarial domain adaptation. In *European Conference on Computer Vision (ECCV)*, pages 135–150, 2018. 2, 3, 7
- [4] Woong-Gi Chang, Tackgeun You, Seonguk Seo, Suha Kwak, and Bohyung Han. Domain-specific batch normalization for unsupervised domain adaptation. In *IEEE/CVF Conference on Computer Vision and Pattern Recognition (CVPR)*, 2019. 2
- [5] Minghao Chen, Hongyang Xue, and Deng Cai. Domain adaptation for semantic segmentation with maximum squares loss. In *IEEE/CVF International Conference on Computer Vision (ICCV)*, 2019. 2
- [6] Xinyang Chen, Sinan Wang, Mingsheng Long, and Jianmin Wang. Transferability vs. discriminability: Batch spectral penalization for adversarial domain adaptation. In *International Conference on Machine Learning (ICML)*, 2019. 2
- [7] Yuhua Chen, Wen Li, Christos Sakaridis, Dengxin Dai, and Luc Van Gool. Domain adaptive faster r-cnn for object detection in the wild. In *IEEE Conference on Computer Vision and Pattern Recognition (CVPR)*, 2018. 1
- [8] Boris Chidlovskii, Stéphane Clinchant, and Gabriela Csurka. Domain adaptation in the absence of source domain data. In *ACM SIGKDD International Conference on Knowledge Discovery and Data Mining (KDD)*, 2016. 2
- [9] Gabriela Csurka. Domain adaptation for visual applications: A comprehensive survey. *arXiv preprint arXiv:1702.05374*, 2017. 1
- [10] Shuhao Cui, Xuan Jin, Shuhui Wang, Yuan He, and Qingming Huang. Heuristic domain adaptation. In *Advances in Neural Information Processing Systems (NeurIPS)*, 2020. 6, 7
- [11] Shuhao Cui, Shuhui Wang, Junbao Zhuo, Liang Li, Qingming Huang, and Qi Tian. Towards discriminability and diversity: Batch nuclear-norm maximization under label insufficient situations. In *IEEE/CVF Conference on Computer Vision and Pattern Recognition (CVPR)*, 2020. 2
- [12] Alexey Dosovitskiy, Lucas Beyer, Alexander Kolesnikov, Dirk Weissenborn, Xiaohua Zhai, Thomas Unterthiner, Mostafa Dehghani, Matthias Minderer, Georg Heigold, Sylvain Gelly, et al. An image is worth 16x16 words: Transformers for image recognition at scale. In *International Conference on Learning Representations (ICLR)*, 2021. 2, 6
- [13] Lixin Duan, Ivor W Tsang, Dong Xu, and Stephen J Maybank. Domain transfer svm for video concept detection. In *IEEE Conference on Computer Vision and Pattern Recognition (CVPR)*, 2009. 2
- [14] Basura Fernando, Amaury Habrard, Marc Sebban, and Tinne Tuytelaars. Unsupervised visual domain adaptation using subspace alignment. In *IEEE International Conference on Computer Vision (ICCV)*, 2013. 2
- [15] Yaroslav Ganin, Evgeniya Ustinova, Hana Ajakan, Pascal Germain, Hugo Larochelle, François Laviolette, Mario Marchand, and Victor Lempitsky. Domain-adversarial training of neural networks. *Journal of Machine Learning Research*, 17(1):2096–2030, 2016. 1, 2
- [16] Ryan Gomes, Andreas Krause, and Pietro Perona. Discriminative clustering by regularized information maximization. In *Advances in Neural Information Processing Systems (NeurIPS)*, 2010. 4
- [17] Boqing Gong, Yuan Shi, Fei Sha, and Kristen Grauman. Geodesic flow kernel for unsupervised domain adaptation. In *IEEE Conference on Computer Vision and Pattern Recognition (CVPR)*, 2012. 2
- [18] Ian J Goodfellow, Jean Pouget-Abadie, Mehdi Mirza, Bing Xu, David Warde-Farley, Sherjil Ozair, Aaron Courville, and Yoshua Bengio. Generative adversarial networks. In *Advances in Neural Information Processing Systems (NeurIPS)*, 2014. 1
- [19] Kaiming He, Xiangyu Zhang, Shaoqing Ren, and Jian Sun. Deep residual learning for image recognition. In *IEEE Conference on Computer Vision and Pattern Recognition (CVPR)*, 2016. 5
- [20] Geoffrey Hinton, Oriol Vinyals, and Jeff Dean. Distilling the knowledge in a neural network. In *NIPS Deep Learning and Representation Learning Workshop*, 2015. 2, 3, 4
- [21] Judy Hoffman, Eric Tzeng, Taesung Park, Jun-Yan Zhu, Phillip Isola, Kate Saenko, Alexei Efros, and Trevor Darrell. Cycada: Cycle-consistent adversarial domain adaptation. In *International Conference on Machine Learning (ICML)*, 2018. 2, 5, 6
- [22] Dapeng Hu, Jian Liang, Qibin Hou, Hanshu Yan, Yunpeng Chen, Shuicheng Yan, and Jiashi Feng. Panda: Prototypical unsupervised domain adaptation. *arXiv preprint arXiv:2003.13274*, 2020. 1
- [23] Weihua Hu, Takeru Miyato, Seiya Tokui, Eiichi Matsumoto, and Masashi Sugiyama. Learning discrete representations via information maximizing self-augmented training. In *International Conference on Machine Learning (ICML)*, 2017. 2, 4
- [24] Jiayuan Huang, Arthur Gretton, Karsten Borgwardt, Bernhard Schölkopf, and Alex Smola. Correcting sample selection bias by unlabeled data. In *Advances in Neural Information Processing Systems (NeurIPS)*, 2006. 2
- [25] Ahmet Iscen, Giorgos Tolias, Yannis Avrithis, and Ondrej Chum. Label propagation for deep semi-supervised learning. In *IEEE/CVF Conference on Computer Vision and Pattern Recognition (CVPR)*, 2019. 4
- [26] Ying Jin, Ximei Wang, Mingsheng Long, and Jianmin Wang. Minimum class confusion for versatile domain adaptation. In *European Conference on Computer Vision (ECCV)*, 2020. 2, 8
- [27] Thorsten Joachims et al. Transductive inference for text classification using support vector machines. In *International Conference on Machine Learning (ICML)*, 1999. 2

[28] Guoliang Kang, Lu Jiang, Yi Yang, and Alexander G Hauptmann. Contrastive adaptation network for unsupervised domain adaptation. In *IEEE/CVF Conference on Computer Vision and Pattern Recognition (CVPR)*, 2019. 2, 5, 7

[29] Mehran Khodabandeh, Arash Vahdat, Mani Ranjbar, and William G Macready. A robust learning approach to domain adaptive object detection. In *IEEE/CVF International Conference on Computer Vision (ICCV)*, 2019. 1

[30] Kyungul Kim, ByeongMoon Ji, Doyoung Yoon, and Sangheum Hwang. Self-knowledge distillation: A simple way for better generalization. *arXiv preprint arXiv:2006.12000*, 2020. 3

[31] Piotr Koniusz, Yusuf Tas, and Fatih Porikli. Domain adaptation by mixture of alignments of second-or higher-order scatter tensors. In *IEEE Conference on Computer Vision and Pattern Recognition (CVPR)*, 2017. 2

[32] Jogendra Nath Kundu, Naveen Venkat, R Venkatesh Babu, et al. Universal source-free domain adaptation. In *IEEE/CVF Conference on Computer Vision and Pattern Recognition (CVPR)*, 2020. 1, 2

[33] Ilja Kuzborskij and Francesco Orabona. Stability and hypothesis transfer learning. In *International Conference on Machine Learning (ICML)*, 2013. 2

[34] Samuli Laine and Timo Aila. Temporal ensembling for semi-supervised learning. In *International Conference on Learning Representations (ICLR)*, 2017. 3, 4

[35] Rui Li, Qianfen Jiao, Wenming Cao, Hau-San Wong, and Si Wu. Model adaptation: Unsupervised domain adaptation without source data. In *IEEE/CVF Conference on Computer Vision and Pattern Recognition (CVPR)*, 2020. 1, 2, 3

[36] Jian Liang, Ran He, Zhenan Sun, and Tieniu Tan. Aggregating randomized clustering-promoting invariant projections for domain adaptation. *IEEE Transactions on Pattern Analysis and Machine Intelligence*, 41(5):1027–1042, 2018. 2

[37] Jian Liang, Ran He, Zhenan Sun, and Tieniu Tan. Distant supervised centroid shift: A simple and efficient approach to visual domain adaptation. In *IEEE/CVF Conference on Computer Vision and Pattern Recognition (CVPR)*, 2019. 2

[38] Jian Liang, Dapeng Hu, and Jiashi Feng. Do we really need to access the source data? source hypothesis transfer for unsupervised domain adaptation. In *International Conference on Machine Learning (ICML)*, 2020. 1, 2, 3, 4, 5, 6, 7, 8

[39] Jian Liang, Dapeng Hu, Yunbo Wang, Ran He, and Jiashi Feng. Source data-absent unsupervised domain adaptation through hypothesis transfer and labeling transfer. *arXiv preprint arXiv:2012.07297*, 2020. 2, 5, 6, 7, 8

[40] Jian Liang, Yunbo Wang, Dapeng Hu, Ran He, and Jiashi Feng. A balanced and uncertainty-aware approach for partial domain adaptation. In *European Conference on Computer Vision (ECCV)*, 2020. 2, 7, 8

[41] Mingsheng Long, Yue Cao, Jianmin Wang, and Michael Jordan. Learning transferable features with deep adaptation networks. In *International Conference on Machine Learning (ICML)*, 2015. 1

[42] Mingsheng Long, Zhangjie Cao, Jianmin Wang, and Michael I Jordan. Conditional adversarial domain adaptation. In *Advances in Neural Information Processing Systems (NeurIPS)*, 2018. 1, 2, 5, 6, 7

[43] Mingsheng Long, Han Zhu, Jianmin Wang, and Michael I Jordan. Deep transfer learning with joint adaptation networks. In *International Conference on Machine Learning (ICML)*, 2017. 2

[44] Zhihe Lu, Yongxin Yang, Xiatian Zhu, Cong Liu, Yi-Zhe Song, and Tao Xiang. Stochastic classifiers for unsupervised domain adaptation. In *IEEE/CVF Conference on Computer Vision and Pattern Recognition (CVPR)*, 2020. 5, 7

[45] Fabio Maria Carlucci, Lorenzo Porzi, Barbara Caputo, Elisa Ricci, and Samuel Rota Bulo. Autodial: Automatic domain alignment layers. In *IEEE International Conference on Computer Vision (ICCV)*, 2017. 2

[46] Sinno Jialin Pan, Ivor W Tsang, James T Kwok, and Qiang Yang. Domain adaptation via transfer component analysis. *IEEE Transactions on Neural Networks*, 22(2):199–210, 2010. 2

[47] Sinno Jialin Pan and Qiang Yang. A survey on transfer learning. *IEEE Transactions on Knowledge and Data Engineering*, 22(10):1345–1359, 2009. 1

[48] Xingchao Peng, Ben Usman, Neela Kaushik, Judy Hoffman, Dequan Wang, and Kate Saenko. Visda: The visual domain adaptation challenge. *arXiv preprint arXiv:1710.06924*, 2017. 5

[49] Kate Saenko, Brian Kulis, Mario Fritz, and Trevor Darrell. Adapting visual category models to new domains. In *European Conference on Computer Vision (ECCV)*, 2010. 5

[50] Roshni Sahoo, Divya Shanmugam, and John Guttag. Unsupervised domain adaptation in the absence of source data. In *ICML Workshop on Uncertainty and Robustness in Deep Learning*, 2020. 2

[51] Kuniaki Saito, Yoshitaka Ushiku, Tatsuya Harada, and Kate Saenko. Strong-weak distribution alignment for adaptive object detection. In *IEEE/CVF Conference on Computer Vision and Pattern Recognition (CVPR)*, 2019. 1

[52] Kuniaki Saito, Kohei Watanabe, Yoshitaka Ushiku, and Tatsuya Harada. Maximum classifier discrepancy for unsupervised domain adaptation. In *IEEE Conference on Computer Vision and Pattern Recognition (CVPR)*, 2018. 2

[53] Tim Salimans and Diederik P Kingma. Weight normalization: A simple reparameterization to accelerate training of deep neural networks. In *Advances in Neural Information Processing Systems (NeurIPS)*, 2016. 3

[54] Rui Shu, Hung H Bui, Hirokazu Narui, and Stefano Ermon. A dirt-t approach to unsupervised domain adaptation. In *International Conference on Learning Representations (ICLR)*, 2018. 5

[55] Masashi Sugiyama, Shinichi Nakajima, Hisashi Kashima, Paul von Bünau, and Motoaki Kawanabe. Direct importance estimation with model selection and its application to covariate shift adaptation. In *Advances in Neural Information Processing Systems (NeurIPS)*, 2007. 2

[56] Baochen Sun, Jiashi Feng, and Kate Saenko. Return of frustratingly easy domain adaptation. In *AAAI Conference on Artificial Intelligence (AAAI)*, 2016. 2

[57] Christian Szegedy, Vincent Vanhoucke, Sergey Ioffe, Jon Shlens, and Zbigniew Wojna. Rethinking the inception architecture for computer vision. In *IEEE Conference on Computer Vision and Pattern Recognition (CVPR)*, 2016. 3, 4

[58] Hui Tang, Ke Chen, and Kui Jia. Unsupervised domain adaptation via structurally regularized deep clustering. In *IEEE/CVF Conference on Computer Vision and Pattern Recognition (CVPR)*, 2020. 5, 6, 7

[59] Antti Tarvainen and Harri Valpola. Mean teachers are better role models: Weight-averaged consistency targets improve semi-supervised deep learning results. In *Advances in Neural Information Processing Systems (NeurIPS)*, 2017. 3

[60] Yi-Hsuan Tsai, Wei-Chih Hung, Samuel Schulter, Ki-hyuk Sohn, Ming-Hsuan Yang, and Manmohan Chandraker. Learning to adapt structured output space for semantic segmentation. In *IEEE Conference on Computer Vision and Pattern Recognition (CVPR)*, 2018. 1

[61] Eric Tzeng, Judy Hoffman, Kate Saenko, and Trevor Darrell. Adversarial discriminative domain adaptation. In *IEEE Conference on Computer Vision and Pattern Recognition (CVPR)*, 2017. 1, 2

[62] Eric Tzeng, Judy Hoffman, Ning Zhang, Kate Saenko, and Trevor Darrell. Deep domain confusion: Maximizing for domain invariance. *arXiv preprint arXiv:1412.3474*, 2014. 1, 2

[63] Hemanth Venkateswara, Jose Eusebio, Shayok Chakraborty, and Sethuraman Panchanathan. Deep hashing network for unsupervised domain adaptation. In *IEEE Conference on Computer Vision and Pattern Recognition (CVPR)*, 2017. 5

[64] Vikas Verma, Kenji Kawaguchi, Alex Lamb, Juho Kannala, Yoshua Bengio, and David Lopez-Paz. Interpolation consistency training for semi-supervised learning. In *International Joint Conference on Artificial Intelligence (IJCAI)*, 2019. 2, 4

[65] Ruijia Xu, Guanbin Li, Jihan Yang, and Liang Lin. Larger norm more transferable: An adaptive feature norm approach for unsupervised domain adaptation. In *IEEE/CVF International Conference on Computer Vision (ICCV)*, 2019. 2

[66] Li Yuan, Francis EH Tay, Guilin Li, Tao Wang, and Jiashi Feng. Revisiting knowledge distillation via label smoothing regularization. In *IEEE/CVF Conference on Computer Vision and Pattern Recognition (CVPR)*, 2020. 3

[67] Hongyi Zhang, Moustapha Cisse, Yann N Dauphin, and David Lopez-Paz. mixup: Beyond empirical risk minimization. In *International Conference on Learning Representations (ICLR)*, 2017. 4

[68] Haojian Zhang, Yabin Zhang, Kui Jia, and Lei Zhang. Unsupervised domain adaptation of black-box source models. *arXiv preprint arXiv:2101.02839*, 2021. 2, 4, 6

[69] Yang Zhang, Philip David, and Boqing Gong. Curriculum domain adaptation for semantic segmentation of urban scenes. In *IEEE International Conference on Computer Vision (ICCV)*, 2017. 1

[70] Zhilu Zhang and Mert R Sabuncu. Self-distillation as instance-specific label smoothing. In *Advances in Neural Information Processing Systems (NeurIPS)*, 2020. 2

[71] Fuzhen Zhuang, Zhiyuan Qi, Keyu Duan, Dongbo Xi, Yongchun Zhu, Hengshu Zhu, Hui Xiong, and Qing He. A comprehensive survey on transfer learning. *Proceedings of the IEEE*, 109(1):43–76, 2020. 1